XII National and y III International

Conference on Engineering Thermodynamics

12CNIT-2022 - FULL PAPER

Spectral Distribution of Solar Radiation under CIE Standard Sky Conditions

Sol García-Rodríguez[1], Ana García Rodríguez[1], Elena Garrachón Gómez[1], M. Isabel Dieste Velasco[1,2], Montserrat Diez Mediavilla[1,2]

[1]Solar and Wind Feasibility Technologies Research Group (SWIFT), Electromechanical Engineering Dept., University of Burgos, 09006 Burgos, Spain.

[2] UIC-022, Junta de Castilla y León. Electromechanical Eng. Dep. EPS. Universidad de Burgos. Avda. Cantabria s/n, 09006, Burgos, Spain.

Keywords: *Ultraviolet radiation, Photosynthetically Active Radiation, Illuminance, Modelling.*

TOPIC: Renewable energies, environmental impact and circularity

1. Introduction

Solar radiation (SR) is the main driver of the planetary energy balance and it is essential in various areas of human activity. In the energy context, particularly in renewable energies, the broadband solar radiation is converted into useful heat or electricity. The interaction of the wavelengths of the visible spectrum of SR (daylighting or illuminance, L, 400-780 nm) with the photoreceptors of the human eye, allows to perceive the world and its colors, and it has influence on mood and circadian rhythms [1]. Daylight is also essential for the improvement in the energy efficiency of buildings and visual comfort [2]. In agriculture, Photosynthetically Active Radiation (PAR, 400-700 nm) is the energy source to trigger photosynthesis which makes possible the production of food and biomass [3]. Finally, Ultraviolet UVR (UV-A, 315-400 nm; UV-B, 280-215 nm) is responsible for a wide variety of photochemical reactions [4], especially its shorter wavelengths have deleterious effects in many biological systems. Despite the obvious interest of the knowledge of the spectral distribution of SR, the number of measurement stations in most areas of the world is scarce. Therefore, the lack of empirically derived data means that PAR, UVR and L, are routinely estimated as a constant fraction of broadband solar irradiance. However, these ratios are affected by atmospheric conditions, mainly due to the absorption and scattering effects of SR across different regions of the spectrum. In this work the variation of the ratios of illuminance, UVR and PAR, on the horizontal plane (LGH, UvGH, PAR) with respect to the broadband solar radiation on the horizontal plane (RaGH) as a function of atmospheric conditions, determined according to the CIE standard sky classification [5], is studied.

2. Materials and method

The experimental campaign, during which the meteorological data were recorded for this study, took place between 1 March 2019 and 28 February 2022 at a meteorological facility located at the Higher Polytechnic School of Burgos University (42º21′04″N, 3º41′20″W, 856 m a.s.l.). A complete description of the meteorological facility may be found in Ref. [6].

Figure 1. Location of the experimental equipment on the roof of the Higher Polytechnic School building at the University of Burgos, Spain.

The following atmospheric variables are measured at the weather station: precipitation, wind speed and direction, atmospheric pressure, ambient temperature and relative humidity. The data are recorded every 30 seconds and the average values of 10 minutes are stored (values used in this work), the data obtained are analysed and filtered according to quality criteria [7].

Table 1. Models of the sensors installed

Type	Units	Model
Precipitation	mm	Campbell Scientific - 52202 Electrically Heated Rainand Snow Gage
Wind	m s^{-1}	Campbell Scientific - 03002 Wind Sentry Set
Pressure	mbar	VAISALA - PTB110
Temperature	ºC	Campbell Scientific - CS215
Irradiance	W m^{-2}	Hukseflux - SR12-T205
Iluminance	lx	EKO - ML-020S
PAR	µmol m^{-2} s^{-1}	EKO - ML-020P
UV 5	W m^{-2}	K&Z - CUV 5

Table 2. Model of Sky-Scanner installed

Model	MS-321LR Sky Scanner
Dimensions (W × D × H)	430 mm × 380 mm × 440 mm
Mass	12.5 kg
FOV	11°
Luminance	0 to 50 kcd/m2
Radiance	0 to 300 W/m2
A/D Convertor	16 bits
Calibration Error	2%

The CIE classification [5] is used to determine the sky type from the luminance data collected by a Sky-Scanner (EKO MS-321LR). This equipment takes measurements of the sky from sunrise to sunset and performs a complete sweep of the sky for 4 minutes, starting a new sweep of the sky vault every 10 minutes. To avoid erroneous measurements, all luminance measurements that do not fall between 0.1 kcd·m^{-2} and 50 kcd·m^{-2} are discarded, following the device specifications. The first and the last measurement of the day (solar height values lower than 7.5º) are also

eliminated. Data are considered valid when, in addition to meeting all the conditions mentioned above, they are present in all the equipment used in the study.

3. Results and discussion

To determine the CIE standard sky types in Burgos during the measurement campaign, a Sky-Scanner has been used [6, 8, 9]. The frequency of occurrence (FOC, %) of each CIE sky type in Burgos is obtained. In Figure 2, it can be seen that the skies with the highest frequency are clear skies, predominantly 13 with a FOC greater than 20%, followed by 11 and 12 type.

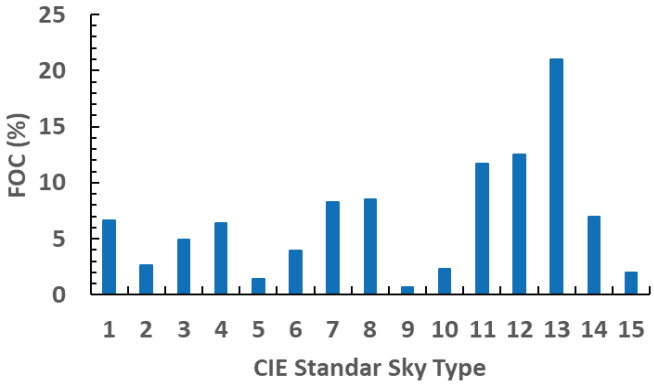

Figure 2. FOC (%) of CIE Standard Sky types in Burgos.

Sky-Scanner devices are not often available at meteorological stations. Thus, to perform the sky classification according to the CIE standard, most authors use a more generic classification which considers only 3 sky categories: overcast, intermediate, and clear skies. According to this classification, the 15 CIE skies are grouped into three categories: overcast from 1 to 5, intermediate from 6 to 10 and clear skies from 11 to 15. A study is made of the frequency of occurrence of each sky type by seasons according to the three categories mentioned, considering spring to the months of March, April and May, summer to June, July, August, autumn to September, October and November and winter to December, January and February. A predominance of clear skies is observed in all seasons with frequencies of 52.4% in spring, 65.5% in summer, 47.8% in autumn, and 42.0% in winter, as shown in Figure 3.

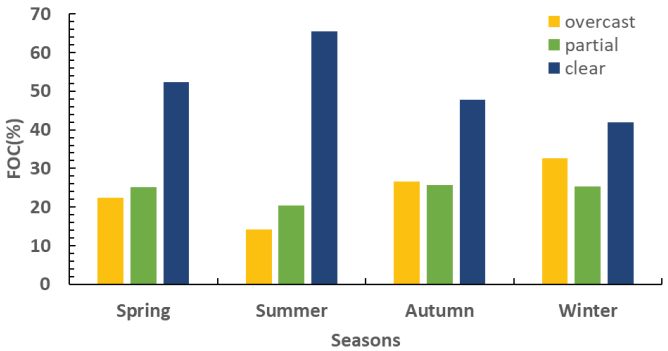

Figure 3. Seasonal FOC, (%) of CIE cloudiness classification in Burgos.

Figure 4, (a), b) and c)) show the high positive correlation between the ten-minute data of the studied variables (LGH-RAGH, UvGH-RaGH and PAR-RAGH) with high values of coefficient of determination (R^2), *i.e.*, 0.995, 0.968 and 0.995 respectively.

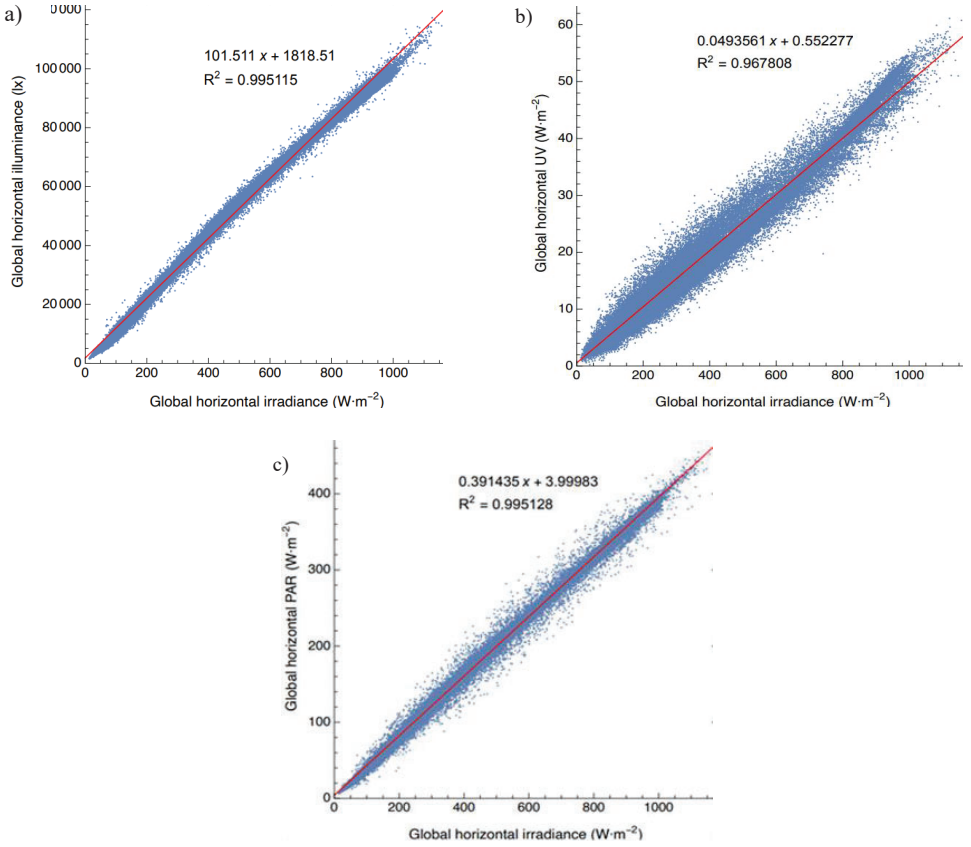

Figure 4.a) LGH vs RaGH (lm/W), b) UvGH vs RaGH (W/m^2) c) PAR vs RaGH (W/m^2) ten-minute data measured in Burgos.

This study also analyzed how LGH/RaGH, UvGH/RaGH and PAR/RaGH ratio varied seasonally during the experimental campaign. Regarding LGH/RaGH ratio, Figure 5 shows that the dispersion in all seasons is very small, being slightly higher in summer. The highest standard deviation (6.39) is recorded in autumn followed by winter and summer, while in spring the standard deviation decreases slightly (5.77). The maximum and minimum values are recorded in autumn (210.93, 62.56 respectively).

The LGH/RaGH ratio during the experimental campaign is 101.5 lm/W.

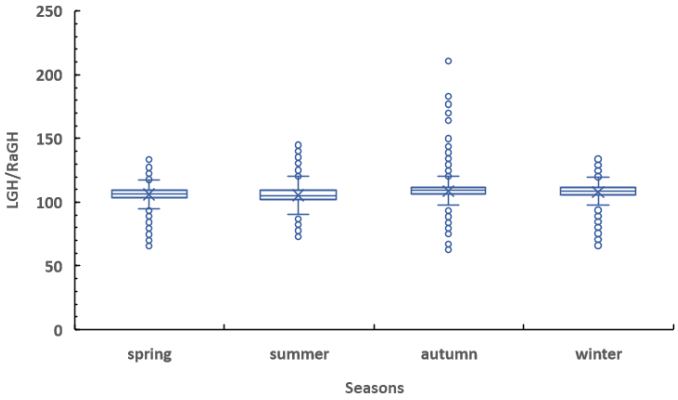

Figure 5. Box-plot ratio LGH/ RaGH for each season.

Figure 6 shows that there is very little dispersion of the UvGH/RaGH ratio in summer, increasing slightly in spring and winter, the greatest dispersion occurs in autumn (in this season the 3 types of skies have a closer FOC). The highest standard deviation (1.12) is recorded in autumn, while in spring and summer the standard deviation decreases to values close to 0.90. The minimum value (0.65) is recorded in summer and the maximum (18.23) in autumn.

The UvGH/RaGH ratio during the experimental campaign is 4.9%.

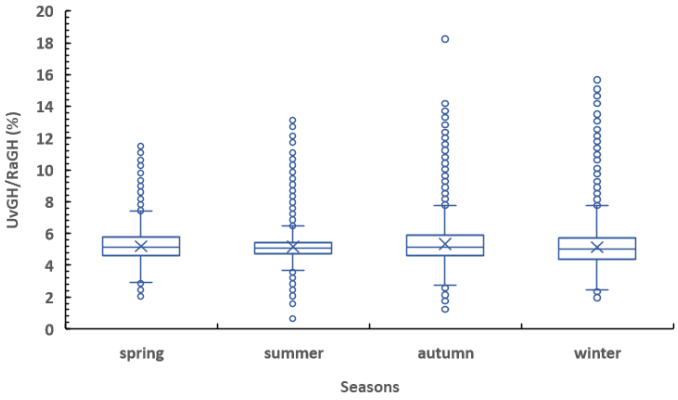

Figure 6. Box-plot ratio UvGH/ RaGH for each season.

Figure 7 shows PAR/RaGH ratio that in summer and winter the dispersion is very small, increasing slightly in spring and autumn. The highest standard deviation (2.68) is registered in autumn, while in spring, summer and winter the standard deviation decreases. The maximum and minimum values are recorded in autumn (80.06 and 18.86 respectively).

The PAR/RaGH ratio during the experimental campaign is 39.1%

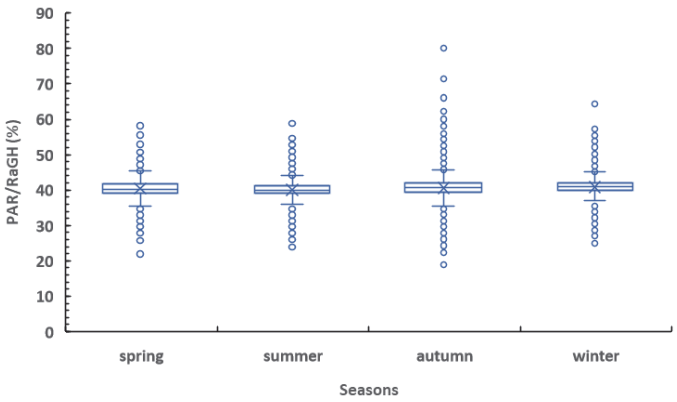

Figure 7. Box-plot ratio PAR/RaGH for each season.

4. Conclusions

In this work, the variation of LGH, UvGH, PAR ratios with respect to RaGH under all sky conditions is studied.
In the city of Burgos, clear skies predominate, being CIE 13 the one with the highest FOC (21%). It can be concluded that clear skies are also predominant in all seasons, reaching higher values in spring and summer.
There is a high positive correlation between the ten-minute data of LGH-RAGH, UvGH-RaGH and PAR-RAGH, with high values of R^2 (0.995, 0.968 and 0.995 respectively).
The LGH/RaGH, UvGH/RaGH, PAR/RaGH ratios during the experimental campaign were 101.5 lm/W, 4.94% and 39.1% respectively.

Acknowledgements

The authors gratefully acknowledge the financial support provided by the Spanish Ministry of Science & Innovation under the I+D+i state program "Challenges Research Projects" (Ref. RTI2018-098900-B-I00). Elena Garrachón-Gómez thanks financial support provided by Junta de Castilla y León (Programa Operativo de Empleo Juvenil, Fondo Social Europeo e Iniciativa de Empleo Juvenil)

References

[1] REA, M. S., M. G. FIGUEIRO, A. BIERMAN AND R. HAMNER Modelling the spectral sensitivity of the human circadian system. Light. Res. Technol., 2012/12/01 2011, 44(4), 386-396.
[2] DIESTE-VELASCO, M., M. DÍEZ-MEDIAVILLA, D. GRANADOS-LÓPEZ, AND D. GONZÁLEZ-PEÑA, et al. Performance of global luminous efficacy models and proposal of a new model for daylighting in Burgos, Spain. *Renewable Energy*, 2019, 133, 1000-1010.
[3] ALADOS, I., I. FOYO-MORENO AND L. ALADOS-ARBOLEDAS Photosynthetically active radiation: Measurements and modelling. *Agricultural and Forest Meteorology*, 1996, 78(1-2), 121-131.
[4] JACOVIDES, C. P., F. S. TYMVIOS, D. N. ASIMAKOPOULOS, N. A. KALTSOUNIDES, et al. Solar global UVB (280–315nm) and UVA (315–380nm) radiant fluxes and their

relationships with broadband global radiant flux at an eastern Mediterranean site. *Agric. For. Meteorol*., 2009/06/15/ 2009, 149(6), 1188-1200.
[5] ISO 15469:2004 (E)/CIE S 011/E:2003 Spatial Distribution of Daylight - CIE Standard General Sky.
[6] SUÁREZ-GARCÍA, A., M. DÍEZ-MEDIAVILLA, D. GRANADOS-LÓPEZ, D. GONZÁLEZ-PEÑA, D. et al. Benchmarking of meteorological indices for sky cloudiness classification. *Solar Energy*, 2020, 195, 499-513.
[7] GUEYMARD, C.A, RUIZ-ARIAS, J.A. Extensive worldwide validation and climate sensitivity analysis of direct irradiance predictions from 1-min global irradiance. *Solar Energy*, 2016, 128, 1–30.

[8] SUÁREZ-GARCÍA, A., GRANADOS-LÓPEZ, D., GONZÁLEZ-PEÑA, D., DÍEZ-MEDIAVILLA, M. et al. Seasonal caracterization of CIE standard sky types above Burgos, northwestern Spain. *Solar Energy*, 2018, 169, 24-33.

[9] GRANADOS-LÓPEZ, D., SUÁREZ-GARCÍA, A., DÍEZ-MEDIAVILLA, M., ALONSO-TRISTÁN, C. Feature selection for CIE standard sky classification. *Solar Energy* 2021, 218, 95–107.